Applicability of geotechnical approaches and constitutive models for foundation analysis of marine renewable energy arrays

Jason E. Heath[a,*], Richard P. Jensen[a], Sam D. Weller[b], Jon Hardwick[b], Jesse D. Roberts[c], Lars Johanning[b]

[a]Department of Geomechanics, Sandia National Laboratories, PO Box 5800, Mail Stop 0750, Albuquerque, New Mexico 87185-0750 USA

[b]Renewable Energy Group, SERSF Building, College of Engineering, Mathematics and Physical Sciences, University of Exeter, Penryn Campus, Cornwall, United Kingdom TR10 9FE

[c]Department of Water Power Technologies, Sandia National Laboratories, PO Box 5800, Mail Stop 1124, Albuquerque, New Mexico 87185-1124 USA

*Corresponding author. Tel.: +1 505 845 1375.

Email address: jeheath@sandia.gov (J.E. Heath).

Abstract

For Marine Renewable Energy (MRE) to become a viable alternative energy source, it must encompass large arrays of devices. Arrays may include 1000s of devices. The associated foundations or anchors may encounter a range of seafloor sediment types and geotechnical properties. Wave and tidal energy convertors induce unique loads on foundations and anchors that are different from other seafloor engineering applications. Thus, there is a need for a combination of advanced site analysis and performance assessment. Geotechnical engineering plays the vital role of ensuring that foundation and anchor systems perform successfully for MRE devices. Our paper reviews the unique frequency and magnitude of loading regimes experienced by MRE arrays. We examine potential loading conditions on the foundation-anchor systems. Loading regimes include environmental and system loads from single devices or arrays

of devices. We present specific load examples from field data. We explore the applicable geotechnical approaches to address these conditions, including constitutive models that may or may not adequately capture the response of the seafloor sediments to the MRE loads. Partial to fully dynamic constitutive model formulations may be necessary to properly model sediment-fluid hydromechanical response to MRE loading. Spacing of full MRE arrays and spatial variability in sediment properties may require multiple foundation types.

Highlights

Keywords: marine renewable energy; geotechnical; foundation; constitutive model; cyclic loading; array

1. Introduction

Commercial-scale marine renewable energy (MRE) systems will involve arrays of devices that secure to the seafloor via foundations or anchors. In order to achieve global installed capacity targets (e.g., 10-20 GW by 2050 in the UK [1]), device arrays are likely to occupy areas up to several square kilometers [2–4] that may span across multiple seafloor environments [5]. These devices will transmit loads to the seafloor sediment, soil, or rock—hereafter referred to as "geomaterials"—which may affect seafloor geomaterial properties and the overall physical performance of an MRE system. Multiple devices may be tethered to a single anchor, thereby creating fully three-dimensional dynamic loading scenarios [4]. Cyclic or periodic loading may induce degradation in stiffness and strength of geomaterials, which may cause potential creep movement of foundations or anchors [6–8]. Liquefaction is also possible under high frequency rapid loading and vibration, especially of cohesionless geomaterials [8].

Experience with fully-deployed commercial-scale arrays tidal- or wave-energy convertors is limited—to date, small-scale arrays and single such devices have been tested [9–12]. Recent

MRE-specific research on arrays focuses on hydrodynamics of tidal and wave MRE systems [2,3,13,14]. Foundation, anchor, and geomaterial response for MRE arrays have received less attention, mainly for offshore wind turbine arrays [15]. Thus, the response and performance of seafloor geomaterials is uncertain, given the combination of potentially large MRE arrays, seafloor heterogeneity, unique loading profiles of tidal and wave energy convertors, and coupled hydromechanical-seafloor behavior. As foundations and anchors represent a primary cost to construction, maintenance, and performance of MRE systems [16,17], success of this new industry depends on accurately predicting and designing the response of seafloor geomaterials.

A major research gap is lack of knowledge on the applicability of currently-available geomaterial constitutive models for the unique loading magnitudes, frequencies, and scenarios of MRE wave and tidal energy convertor arrays. Geotechnical approaches and constitutive models were not originally developed for the unique MRE scenarios, and thus should be assessed for their applicability. To address this gap, this paper reviews the offshore structure and MRE-related literature, augmented with novel loading information from deployed MRE systems (see Section 2). The objective is to generate knowledge on what geotechnical approaches and constitutive models are available, suited, and preferable for capturing the seafloor geomaterial heterogeneity and response under MRE loading conditions (see Section 3). The paper discusses what future work is needed—including laboratory, field, or numerical modeling—to evaluate or develop appropriate geotechnical approaches and constitutive models if they do not currently exist (see Sections 3 and 4). Geologic heterogeneity is also addressed in the context of variability of seafloor geomaterial properties and the potential size of MRE arrays, which in turn may affect the uniformity, robustness, or mix of different foundation-anchors systems or MRE devices that may be needed for a single site.

2. Frequency and Magnitudes of MRE-induced Loads

The magnitudes, frequencies, and number of loading cycles experienced by MRE foundations and anchors are specific to both the operational requirements of the device, the type of mooring, anchoring, or foundation system employed, as well as the site location. Loads can be broadly classified as follows: static loading (e.g., due to mooring line pretension); long-term cyclic loading (e.g., during operational and storm conditions); and impulse loading. Seismic loading, a form of impulse loading, may also be important in areas prone to earthquakes. These types of loading all fall under different assumptions for modeling stress-strain and geomaterial response, including the coupled hydromechanical processes owing to the fluid that fills the pores of the porous geomaterials and the type of loading, which will be addressed in detail in Sections 3 and 4. For simplicity, in Section 2 we organize information on environmental loads, systems loads, and load characteristics of arrays of MRE systems, which may manifest the aforementioned static, cyclic, and impulse loading to varying degrees (Table 1).

2.1 Environmental loads

Most loads that are applied directly to the MRE structure or device originate from the combined effects of wind, waves, and current [18,19]. These three load sources are rarely co-linear in direction at any one time. For floating devices or sea surface-piercing structures the orbital motion of waves imparts loads at first-order (e.g., typically 5–20 s), second-order, and higher-order frequencies. The magnitude and frequency of wave loading is dependent on a multitude of factors including incident wave characteristics (e.g., significant height, peak period, spectral shape, and directionality), device size, water depth, and bathymetry [2,20]. Research has shown that second-order wave loads (which are associated with steady mean drift loads and cyclic drift motions at sum- and difference- frequencies) should be considered for floating wind

turbines [21], and these loads will also be important for MRE devices [22]. The decay of wave particle velocities with depth (d) means that seabed-mounted devices are less susceptible to wave loading in deep water (i.e. $d/L > 0.5$, where L is wavelength [23]). Devices located in shallow water are affected by refraction and shoaling, where horizontal wave loads increase as progressive waves become steeper in profile. It is possible that breaking or slamming waves can lead to impulse (short duration and large magnitude) loads on floating devices and surface piercing structures. Wilkinson et al. in [24] reported experimental model tests of a bottom-mounted hinge type wave energy converter. When comparing the responses of solid and modular type flap structures, it was noted that while the measured surge-load time-series were similar, significant differences occurred in loading of the foundation in the yaw and roll directions (reductions of 43% and 28%, respectively, for the modular structure). For wind turbine monopiles, it has been demonstrated that breaking waves lead to an amplification of the foundation overturning moment [4,25]).

Many coastal locations experience multiple tides during each 24 hour period. The change in surface elevation will alter the mooring line pretension of floating devices and for fixed structures also change the distribution of applied wave and current loads. In each case this is likely to (albeit temporarily) alter the response harmonics of the floating device structure. The lay-down and uplift of the mooring lines of catenary mooring systems from the seafloor will also be affected by the change in device position. During the tidal cycle the current velocity varies from zero (slack tide) to peak (ebb or flood depending on the direction), with the highest velocities usually measured at the surface. In extreme cases, vortex-induced vibration can cause high frequency loading to support structures and scouring [26] in addition to mooring lines or umbilical cables [20]. Complex loading may also occur in turbulent flows [13].

For surface piercing structures or floating devices, wind also creates another load component of varying magnitude (e.g., wind gusts) and direction that is dependent on the size and shape of the exposed device. Devices that have large areas exposed to the wind will clearly sustain considerable loads in high wind velocities, which will be transferred to the foundation (i.e., mudline bending moment, [27]), or in the case of a floating device, mooring lines and anchors. Even in steady wind conditions the level arm caused by wind loading of the rotor could cause platform rotations [28] leading to unequal loading of the anchoring points. Intermittent impact from ice flows or marine life and the effects of biofouling may also need to be considered if relevant to the site [29,30]. Combinations of extreme conditions are typically used to ensure that a design is sufficiently robust and detailed dynamic analysis is typically carried out (e.g. [68]). While preliminary guidelines for MRE devices have been developed (e.g., [31]), many refer back to existing offshore certification guidance. For example, DNV-OS-E301 states 100-year return periods for wind and waves with 10-year return period for current for Norwegian and UK sectors [30]. In addition a 50-year return period for water level may also be used [32]. Maintaining anchor or foundation integrity during storm conditions is particularly important as highly variable cyclic loading will occur.

2.2 System loads

In addition to environmental loads applied directly to the device, the mooring system, foundation, or anchor loads are also dependent on the motions of the device and/or power take-off (PTO) system. Snatch loading occurs when slack lines are rapidly loaded as a result of dynamic device motions (e.g., as a steep wave passes [33]). Wave energy converters (WECs) are designed to harness the predominant wave characteristics through passive or active tuning. The response of the device may therefore be close to resonant in one or more modes of motion and in

extreme cases large motions may lead to significant slamming forces on the structure [34] and the subsequent amplification of loads transmitted to the anchors through the mooring system.

In steady-flow conditions, tidal turbine foundations are likely to experience loads and overturning moments that correspond to rotation and blade passing frequencies. In addition floating turbines may experience gyroscopic coupling between turbine rotation and device motions akin to floating wind turbines [28]. Other harmonics, originating from power take-off subsystems (i.e., gearboxes) are also likely to be transmitted to the foundation through the support structure. The variation of current velocity over a tidal cycle will alter the steady-thrust load applied at the nacelle [35] and to the support structure. Current velocities are depth dependent and profiles alter throughout the tidal cycle (Figure 1). Furthermore in unsteady-flow conditions, local flow fluctuations (i.e., the interaction between blade tip vortices and shedding from the support structure) causes thrust coefficients to oscillate [36]. The interaction between several complex wake profiles from multiple devices in an MRE array is likely to introduce further velocity fluctuations across an array [13].

2.3 Load characteristics of MRE arrays

MRE array devices are subjected to several key loading regimes, which should be considered during anchor and foundation design and predicting geomaterial response. The rationale behind placing devices in array layouts is three-fold: 1) for ease of access to carry out installation, maintenance, and decommissioning operations; 2) to reduce cost through shared infrastructure (e.g., for power transmission, mooring, or foundation subsystems); and 3) to influence the response of the devices based on the hydrodynamic interactions occurring between devices. The effect of positioning multiple fixed or floating devices in close proximity on array power production has been well studied for both wave and tidal energy devices in order to take

advantage of constructive interactions [37] (or at least minimize destructive interactions) and to study wake interaction effects [38]. Several theoretical and experimental studies have proposed device separation distances for WECs to optimize energy conversion from these effects. Recent research by Babarit identified that for distances greater than 10× the device diameter the power production benefit of array layouts diminishes [39].

The hydrodynamic response of closely spaced devices is complex due to the interaction between the wind, surface current, and incident, scattered, and radiated wave-fields. For devices that are interlinked and/or use shared connection points the complexity of anchor or foundation loading is further compounded by the dynamic response of multiple interacting bodies [40]. In extreme cases snatch loading could occur if the motion of neighboring devices is markedly different. Such systems are characterized by highly variable and multi-directional loads that differ from individual devices [41]. To date the only shared-foundation systems in existence are fixed foundation structures, for example WaveStar Energy's Wave Star [39,42].

2.4 Load examples

The South West Mooring Test Facility (SWMTF) and Fred Olsen BOLT "Lifesaver" wave energy device have been deployed in Falmouth Bay, UK. Owned and operated by the University of Exeter, the SWMTF is a highly instrumented buoy, which provides a floating platform for in-situ testing of mooring and umbilical components and systems ([43], Figure 2a). The SWMTF allows the dynamic response and mooring tensions of buoy-like equipment to be assessed and compared to incident wind, wave, and current conditions. The mooring system comprises three chain and nylon rope [12] catenary lines (Figure 2b) with axial tensions measured at each fairlead at a sample rate of 20 Hz. A large body of research has stemmed from measurements recorded by the SWMTF since it was commissioned in 2009 including studies

investigating the effect of different mooring system configurations (e.g. [44,45]). Adjacent to the SWMTF is a four beam Acoustic Doppler Current Profilers (ADCPs) (mounted on the seabed 27 m below chart datum), which is used to obtain directional wave and current measurements for peak load characterization [46] and numerical model calibration with nearby wave buoys [47].

The Fred Olsen BOLT Lifesaver device was deployed at the FaBTest site in Falmouth Bay during April 2012 [48]. The device has an annulus structure supporting three power take-off units which react with the seabed via taut mooring lines (Figure 2c). An additional five catenary mooring lines provide restraint during storm conditions, and for each line fairlead tension measurements are recorded at a sample rate of 20 Hz. A SeaWatch wave buoy is used to measure wave surface elevations adjacent to the BOLT Lifesaver device.

The magnitude, frequency, and number of cycles experienced by the anchors used on the SWMTF and BOLT Lifesaver device can be inferred from the mooring line tensions measured by each device. Two intervals lasting seven days have been selected from the first deployment of the SWMTF [12,49] during September and November 2010. These intervals are of interest because the SWMTF was subjected to relatively calm (21–26 September 2010) and mild-storm (14–21 November 2010) conditions (Figure 3). Referring to Figure 2b, rainflow analysis was conducted on mooring tensions for lines 1 and 2 using version 2.2.1 of the Wave Analysis for Fatigue and Oceanography (WAFO) Toolbox [50] in Matlab®. The rainflow diagrams plotted in Figure 4 illustrate the difference in loading conditions experienced by the mooring system of the SWMTF in moderately calm and mild-storm conditions. Focusing on load ranges greater than 0.2 kN the number of load cycles experienced by each line is similar for each interval (Table 2). However, the distribution of cycles differs for each interval, with a greater spread of load ranges noted during the November interval, with loads of up to 52 kN measured. Comparison of the

spectral distribution of load frequencies using Fast Fourier Transform analysis also reveals differences between the two time intervals, with the mild-storm tensions biased towards lower frequencies (Figure 5). This bias appears to correspond with the spectrum obtained from ADCP surface elevations measured during the mild-storm interval (Figure 5). This is probably due to the influence of the long-period swell for frequencies below 0.1 Hz. The higher frequencies (>0.3Hz) may be due to locally generated wind waves.

These results demonstrate that MRE mooring loads are highly variable: of varying periodicity, magnitude, mean load, and timescales. Rainflow analysis was also carried out on the load measurements recorded from the BOLT Lifesaver WEC (Figure 6). The analysis shows the cycles recorded on all mooring limbs from 24–29 January 2013. A wave buoy has been located close to the BOLT device and is continually recording the sea state conditions at the site, the significant wave height, wave period, and direction for the 24–29 January 2013 are shown in Figure 7. The spectral mooring line distributions show similar patterns, but of varying magnitude (Figure 8).

3. Geotechnical Approaches, MRE Loadings, and Array Spacing

3.1 Seafloor Heterogeneity and MRE Spacing

A commercial-scale MRE array will likely encounter a variety of seafloor geomaterials. Proposed tidal and wave energy convertor arrays may be up to several square kilometers in size [2–4], increasing the probability of crossing differing geologic environments [5]. Seafloor geomaterials, ranging from sand to clay with a variety of bedforms (e.g., subaqueous dune fields) add complexity to the transmission of MRE loads via foundations and/or anchors to the host geomaterials. Many studies fail to account for seafloor heterogeneity while studying the energy and hydrodynamic performance of MRE systems and arrays (e.g., [2,3,13]). Recent work

indicates that geologic heterogeneity of seafloor geomaterials and bedforms may impact array layouts, design, and performance. Barrie and Conway [5] present seabed characterization results for potential tidal-, wave-, and wind-energy MRE resources for the Pacific offshore of Canada. Their results indicate that subaqueous dune fields, coarse-grained sand to muddy sand, mobile gravel lag, boulder pavements, and sediments of finer-grained silty-sand and clay sediment, underneath the lag surfaces—a result of a combination of climatic and eustatic sea level change and tectonic processes for their particular site—can greatly impact local site development for MRE. The impact on large arrays stems from seafloor geomaterials that necessitate particular foundation or anchor types. Soft to stiff clay or mud, sand, and hard rock may all require specific anchors or foundation types to be most effective [51]. Thus, seafloor heterogeneity for a site means that a single-foundation-or-anchor-type-fits-all approach may not be viable. Figure 9 presents a graphical link between seafloor geologic environments, to geotechnical engineering parameters and foundation and anchors types—reflecting the geologic control on choice of foundation-anchor systems.

Current literature does not have a comparison between the scale of spatial heterogeneity of seafloor geomaterials and proposed spacing of large MRE arrays. Tools for spatial analysis are available, but sparse data at potential MRE sites may limit current efforts to quantify heterogeneity. Also, as Section 2 indicates, load magnitudes have predominant directions. Seafloor geomaterial may also exhibit anisotropic properties due to sediment depositional processes in addition to spatial heterogeneity. The heterogeneity or spatial auto-correlation of sediment properties may be needed to be quantified at the locations of potential MRE arrays to determine whether array sizes are likely to cross multiple sediment types. If the correlation length of the range of a semivariogram [55], which is a measure of spatial heterogeneity, of

seafloor geomaterials at a given site is shorter than MRE array spacing, then devices in an array may encounter different geomaterial types (e.g., sand and clay). If array spacing is within the correlation length, then neighboring devices will fall within seafloor materials that have properties similar to each other. These issues also apply to mooring lines that may lie on the seafloor and experience occasional lift-off from the seafloor. Mooring lines (or energy transmission cables) may cross several seafloor sediment types, affecting the composite effective friction felt by the mooring line. Lift-off of the lines (see Section 2) may remove the line from a particular sediment type thus changing the friction and balance of forces. This will depend on the spatial structure of a given site, which can be captured in part by semivariogram analysis, which has yet to be available in the literature for the different geologic environments of continental shelf that are of interest to the MRE community. In general, anchors or foundations may require design features commensurate with specific sediment types and geotechnical properties (see Table 1.3–5 of [51]).

As an example relating spatial heterogeneity to potential MRE array size, we cite semivariogram data from Goff et al. [56] from the offshore New Jersey middle and outer shelf. This area contains stiff clays to muddy sands and well-sorted medium sands, with gravel patches in several places. The range or distance of spatial correlation for acoustic velocity (in sediments) and mean sand grain size of the computed semiovariogram (based on grab samples and acoustic measurements) is ~12.6 km. Neighboring locations within 12.6 km have variance in properties less than the total variance over the entire studied domain (see Figure 12a of [56]); however, there are still significant variation in properties up to the range. For size comparison, Ahmadian et al. [2] proposed a tidal MRE array with length scale of approximately ~ 6 km by ~ 1.2 km (~ 50 m spacing between devices). Thus, large array sizes may probably encounter different

sediment types and may necessitate multiple anchor or foundation types. A favorable option could be to have a robust anchor or foundation type that is commensurate with multiple seafloor geomaterials.

3.2 Geotechnical Approaches and Correspondence to MRE Arrays and Loads

Recent work investigating the effect of tidal turbine MRE arrays on sediment transport indicates turbines can alter flow patterns and cause localized scour around seafloor structures, possibly leading to structural instability of the foundation [57]. Sediment transport can be affected far (i.e., 15 km) from turbine arrays [2]. Altered patterns of flow within an array may lead to different loads on foundations and/or anchors depending on their position in the array. This adds further complexity to the spatial interaction of arrays with the underlying geological seafloor heterogeneity. Turbines transmit cyclic loads to the foundation-anchor system, and thus if the hydrodynamics vary due to downstream wake effects, then the loading on the foundation-anchors will also vary. Loading may be in part a function of the location of a foundation or anchor in a full-scale array of many devices. Foundation and anchor design may therefore need to address array size and local load distribution within an array. Variability in loads in an array may lead to a possible "weakest link" foundation or anchor location (i.e., the location of the greatest load), which should be designed to better withstand the locally higher loads or weaker geomaterial properties that lessen performance compared to other foundation-anchors in the area. Cascading failure caused by an initial single failure within an array is a possibility. The wind power industry may offer analogous examples of how to cope with different loads and foundation response due to placement of a device within a large array. The understanding of wakes and the technology for wind farms is better developed, and thus estimates for downstream distances of wake effects are available. Bahaj and Myers [13] state that the near wake region of a

wind energy turbine dissipates within 4-5 rotor diameters downstream. The literature does not yet provide established distances of wake effects for tidal energy convertors from field measurements—there have been a number of numerical and small-scale experimental studies on wakes (e.g., [58]). The technology is still in its infancy for full-scale industrial deployment [1].

Section 2 indicates the cyclic nature of MRE loading, including metrics for capturing periodicity of loads, their peaks, and spectral characteristics. Constitutive models for seafloor geomaterial behavior thus need to capture the self-weight (gravity forces) of the foundation and anchors and the overlying and surrounding sediments (e.g., for drag embedment anchors), along with the hydrodynamic loads induced from the waves, currents, and the dynamics of loading from the MRE devices. Earthquake loading with failure modes such as liquefaction may also occur (causing global failure in contrast to the cascading failure scenario presented above). Boundary conditions become important to properly analyze the transmission of loads from the anchors-foundations to the sediment, which can be treated in various ways for cohesionless or cohesive soils [7,51]. Seafloor geomaterial response during installation including vibration, compaction, and other phenomena may also be of concern [51].

Seelig [8] describes the following three categories of cyclic loading for direct-embedment anchors: 1) cyclic line loadings and subsequent loss in strength of seafloor sediment immediately surrounding the anchor; 2) cyclic line loadings that cause accumulated movement or creep of anchors into shallower sediments, resulting in loss of short-term static holding capacity; and 3) earthquake-induced loading that causes loss in sediment strength and anchor failure.
The impact on sediment strength due to cyclic loading is dependent on the time-scale of pore fluid flow in the sediments and the dissipation of excess pore pressure. If pore water drainage cannot occur quickly enough under the cycles of loading, the undrained shear strength will

control sediment failure. Stiffness and strength degradation can also occur as deformation accumulates due to repeated loading and unloading [7,59]. Interaction of excess pore pressure between devices in an MRE array may be a possible concern, which would depend on device and anchor-foundation spacing, the magnitude of excess pore pressure, and sediment permeability—this effect is probably minor as motions from loading probably would not cause much increase in pore pressure for typical MRE systems that is large enough to travel and interfere between devices. Seelig [8] describes loss in strength due to anchor creep as dependent on sediment type, state, and the type of cyclic loading. Another major concern for cyclic loading in general is liquefaction or the condition of excess pore pressure under which sediments lose strength and behave like a liquid [7,59,60]. Liquefaction may need to be considered during foundation or anchor emplacement. During cyclic loading, without sufficient dissipation of excess pore pressure, liquefaction is a possibility in relatively low permeability sediments in the region near a device. Sediment characteristics that mitigate cyclic-induced strength loss include [8]: denser sediment (i.e., relatively higher unit weight); higher yield strength and strain-hardening behavior; lower magnitude of cyclic loading; and lower frequency of total load cycles over the device lifetime.

Possible loading cases for floating and fixed MRE devices are given in Table 3 (also see [54]), including information for devices tethered or attached to single or multiple foundations. The set of loading scenarios results in a range of seafloor sediment responses that affect both the stress-strain behavior of the geomaterials, including possible change in properties through strength or stiffness changes via cyclic loading (load and partial reload-unload-reload cycles), and fluid transport with coupled geomechanical affects for drained, undrained, and partially drained conditions due to the competition of pore pressure buildup, fluid transport controlled by

permeability, and the loading cycles and intensities. Constitutive models therefore need to cover the possible static to dynamic load cases (with the latter including a range of loading frequencies necessary to account for coupled pore pressure-geomechanical behavior).

Recent rigorous approaches for capturing complex hydromechanical behavior of geomaterials under cyclic loading associated with offshore structures are presented by Stickle et al. [7] and Cuellar et al. [6]. These authors emphasize the need for capturing gravity forces (of the geomaterials themselves and the offshore structure), the hydraulic forces, and possible earthquake loading. Excess pore pressure and stress-strain behavior are captured through a set of coupled equations that arise out of generalized Biot theory and general plasticity theory. Excess pore pressure is estimated through these approaches from cyclic loading, which in turns affects the strength degradation. Generalized Biot theory results in formulations that range from those that include dynamic-inertial terms with few assumptions (the *w-u-*p_w formulation, where average relative displacement of fluid to the sediment skeleton, sediment skeleton displacement, and the pore water pressure are the governing variables, respectively) to those that neglect convective acceleration terms of pore water relative to the geomaterial skeleton (the *u-U* formulation, where sediment skeleton displacement and total pore fluid displacement are the governing variables), to those where the whole acceleration of pore fluid relative to geomaterial skeleton is neglected (the partial dynamic *u-pw* formulation—where the governing variables of the system are absolute displacement $\boldsymbol{u}$ of the solid phase and the pore water pressure p_w [6]).

A key metric for the treatment of geomaterial response in terms of static to dynamic behavior is the loading frequency. The connection of what model to use is the frequency of loading, as the different hydromechanical approaches depend on how quickly excess pore pressure is built up or dissipated. Stickle et al. [7] and Zienkiewicz et al. [61] suggest that partial

dynamic formulation is needed for periods of loading in the range of 0.1–0.5 s, which is smaller than most of the periods of the examples in Section 2 (e.g., See Figure 5). Cuellar et al. [62] recommend the partial dynamic u-p_w model formulation (see [61]) for loading frequency cases similar to 0.1 Hz (10 s period), which is the range of the MRE examples of Section 2. Thus, the partial dynamic formulation seems appropriate to capture the coupled hydromechnical response for MRE systems (at least those described in Section 2). Note, however, that Stickle et al. [7] discuss with systems with complex geometries and materials that may experience variable frequencies of loads and thus suggest assessments with both the u–U and u–p_w formulations. They state that if the discrepancy between solutions is less than 3%, then the u-p_w formulation is recommended; otherwise, the u–U formulation may be considered as the pore fluid acceleration may need to be properly accounted for.

The stress-strain constitutive models need to capture the behavior under cyclic loading, which can include contraction in the case of cohesionless geomaterials [62]. Classical plasticity theory models (von Mises, Druker-Prager, or Cam-Clay) do not capture plastic deformation caused by cyclic loading [7]. A variety of other options are available including modified Cam-Clay, plasticity models with isotropic-kinematic hardening, bounding surface models, bubble models, and Generalized Plasticity models. Stickle et al. [7] and Cuellar et al.[6] favor Generalized Plasticity models as they explicitly include effects of multiple load-reload-unload paths. Due to the complexity of MRE loading (see Section 2), modeling that represents complex geomaterial behavior is probably needed. Additional complexity resides in treatment of boundary conditions between foundations and/or anchors and the surrounding geomaterial. Options demonstrated in [6] include no-tension joint elements, which allows gaps to open in cohesive geomaterials and tangential slip (with no opening) for cohensionless geomaterials.

When using numerical methods to model offshore structure-seafloor interactions, the constitutive relations (or models) of marine sediment response are of prime importance—even more so than the particular modelling software used, as poor results will be obtained if an inappropriate constitutive model is used, regardless of the modelling code. To constrain the summary of information from the literature, we focus mainly on constitutive models that can accommodate MRE-related phenomena, including the following: cyclic loading and associated changes in material properties, large strain ranges (e.g., for structure embedment or *in situ* cone penetration testing), liquefaction, layered sediments, and cohesive and cohesionless sediments (Table 4). Sophisticated numerical analysis, at the very least, may require these types of material models. Stickle et al. [7] strongly emphasize the need of an appropriate constitutive model to capture sediment or soil response for marine foundations or structures. They identify cyclic loading as the principle feature of an appropriate constitutive model. The constitutive model should capture the non-associative plasticity of the geomaterials. Stickle et al. [7] list a variety of approaches to improve upon classical plasticity theory models, including the re-modified Cam-Clay model, isotropic-kinematic hardening plasticity models, bounding surface models, bubble models, and generalized plasticity models. They prefer generalized plasticity models because yield or potential surfaces are not explicitly defined, but rather use gradients in those functions and because of the combination of simplicity and accuracy of these models. Table 4 presents several constitutive models of sediment response to loads from offshore structures, with literature sources for cyclic loading and large strain examples [7, 59, 60, 63-71]. In contrast to sophisticated hydromechanical constitutve models of Stickle et al. [7] and Cuellar et al [6], simpler models are summarized by Seelig et al. [8] that estimate the maximum cyclic load with no pore pressure dissipation that can be sustained by the strength of the geomaterial. Approaches

need to capture evolving degradation of strength for the many cycles and complex history of cycles discussed in Section 2.

Assessment of geomaterial response to complex loading profiles, for realistic geologic heterogeneous seafloor environments, would require sophisticated numerical modeling. Commercial numerical codes are mainly suited for running on desktop computers and/or typical engineering workstations. Simulations with commercial codes are by design limited to problem sizes on the order of hundreds of million degrees of freedom, or so. This allows for simulating the sediment and a single device or structure. However, MRE studies may require very sophisticated simulations, such as those tackling some of the problems listed above, including: full spatial (and temporal) heterogeneity in fluid flow and mechanical properties; complex geometries of a variety of interfaces (e.g., device-sediment, device-seafloor); and full-scale, entire MRE device arrays of up to 1000s of devices. Only massively parallel architecture and software specifically designed for such architectures can handle such problems with complex heterogeneous multiphysics. These massively parallel systems may accommodate more degrees of freedom than can be handled by the commercial codes by several orders of magnitude. Systems such as these are generally only available at some governmental institutions and large companies in the oil and gas industry.

Although commercial software may have certain specific coupling capabilities (e.g., Abaqus/Aqua capabilities in Abaqus/Standard to model wave, buoyancy, current and wind loading), full coupling of computational fluid dynamics of open ocean water interaction with mooring systems, the device operation, and the sediment-foundation-anchor interaction is probably beyond current computational abilities. Thus, loads for seafloor material-foundation-anchor interaction require boundary conditions from other sources, such as separate simulations

by other methods for the loads or measurements from the field. While not ideal as this will not account for coupled effects (e.g., device-mooring line-anchor-geomaterial behavior), it may be advantageous for the foundation and/or anchor designer in that it permits the focus to remain on the foundation and/or anchor analysis and design. It needs to be emphasized that there are a number of numerical software solutions, both commercial codes as well as academic codes that can adequately model offshore sediments under a cyclic loading regime that would be applied as a result of the interaction between an MRE foundation or mooring. However, it is of the utmost importance that appropriate constitutive models be utilized in the numerical simulation. Full array simulations, to investigate impacts of heterogeneity of the performance of foundation-anchor system, would require massively parallel computer architecture.

3.3 *In Situ* Field or Laboratory Testing for Parameterizing Constitutive Relations

The constitutive models require parameterization or material parameters to properly represent the sediment or rock response. This is a primary input for the numerical modelling, in addition to boundary conditions and geometrical considerations. Such parameterization typically requires data to be collected from *in-situ* field testing or, probably most commonly, from laboratory testing of sophisticated sediment response behavior. The initial stress state may also be required. The number of parameters depends on the particular constitutive model (see Tables 4 and 5, showing that some require 8 and as many as 15, for the examples given). For example, the Hu et al. [64,65] bounding surface plasticity model requires four parameters related to critical state soil mechanics and four for the hardening modulus. Table 5 summarizes a subset of the constitutive models of Table 4 that capture cyclic sediment response, with listing of the parameters needed and the types of laboratory or field testing required.

Geotechnical laboratory testing can be labor intensive, involving many samples and stress paths. Testing may involve the following (also see Table 5): cyclic simple shear and cyclic triaxial (or truly triaxial) with loading-unloading-reloading paths; reduced triaxial compression; measurement of pore-water-pressure; or centrifuge or shaking table sediment response measurements. A complete discussion of specific parameters and associated tests is beyond the scope of this review; we simply note that sophisticated numerical modelling may involve commensurate sophisticated laboratory or field testing. We also note that geologic materials can be very spatially heterogeneous, depending on the geologic environment. A very involved (and potentially expensive) field sampling and laboratory testing plan may be required to capture heterogeneous properties necessary for numerical modelling that incorporates spatially varying properties.

4. Conclusions and Recommendations

We present the following conclusions and recommendations:

- The geomaterial-MRE device interaction in any array, or in other words, the coupling or interference of geomaterial response due to proximity of neighboring MRE devices is probably not a concern due to pore pressure effects. Because anchor and foundation spacing appears to be on the order of 10s of meters or more, pore-pressure buildup and creep (movement of devices) will be very local and not impact neighbors.
- MRE arrays may cross multiple seafloor geomaterial types. A major question with economic, operational, and maintenance-related ramifications is whether MRE arrays can use only one foundation or anchor type, or whether multiple anchor or foundation types may be required within an array due to widely varying sediment types. Engineers may

consider designing robust foundation-anchor types that can perform well for the given full spatial range of geologic seafloor heterogeneity of a site.

- Geologic seafloor heterogeneity, and spatial-temporal variation in loading profiles of a large array, may pose a potential "weakest link" or location where loading is highest and the geomaterial is the weakest. Such weak points must be identified and designed for to avoid potential cascading—namely failure of a single device in an array that then affects neighbors.
- Global loss in strength of an entire array probably will not occur under typical or even storm loading conditions (or peak storm loading can be designed for). Earthquake loading could be a possible mechanism for such global failure—for example, through large-scale liquefaction.
- For loading frequency cases similar to the example cases of MRE systems (see Section 2), the partial dynamic (u-p_w) model formulation for representing the sediment-fluid hydromechanical response may be appropriate. The fully dynamic u-U formulation may also be considered in cases where pore fluid acceleration may be important (see Section 3.2).
- A variety of constitutive models exist that can capture the salient features of geomaterial-MRE device interaction. Commercial software and approaches can accommodate such models. However, numerical simulation of large-scale arrays with realistic seafloor geomaterial property fields is a challenge, requiring massively parallel computing architecture. Such modeling has not yet been performed in the literature to assess performance of full-scale MRE arrays.

Acknowledgements

J.E. Heath, R.P. Jensen, and J.D. Roberts were supported by the Wind and Water Power Technologies Office of the U.S. Department of Energy's Office of Energy Efficiency and Renewable Energy. This work is an outgrowth of the D4.2 report on foundation-anchor analysis for MRE systems, which was written under the guidance of the Optimal Design Tools for Ocean Energy Arrays (DTOcean) project, a collaborative project funded by the European Commission under the 7th Framework Programme for Research and Development. S.D. Weller, J. Hardwick and L. Johanning were supported by the DTOcean project. The authors would like to thank Fred Olsen Renewables for permitting us to use BOLT Lifesaver data in this paper. Sandia National Laboratories is a multi-program laboratory managed and operated by Sandia Corporation, a wholly owned subsidiary of Lockheed Martin Corporation, for the U.S. Department of Energy's National Nuclear Security Administration under contract DE-AC04-94AL85000.

References

[1] Energy Technologies Institute (ETI) and the UK Energy Research Centre (UKERC). Marine Energy Technology Roadmap 2014. <http://www.eti.co.uk/wp-content/uploads/2014/04/Marine-Roadmap-FULL-SIZE-DIGITAL-SPREADS-.pdf>, 2014.

[2] Ahmadian R, Falconer R, Bockelmann-Evans B. Far-field modelling of the hydro-environmental impact of tidal stream turbines. Renew Energy 2012;38:107–16.

[3] Funke SW, Farrell PE, Piggott, MD. Tidal turbine array optimisation using the adjoint approach. Renew Energy 2014;63:658–73.

[4] Ricci P, Rico A, Ruiz-Minguela P, Boscolo F, Villate JL. Design, modelling and analysis of an integrated mooring system for wave energy arrays. In: Proceedings of the 4th International Conference on Ocean Energy. Dublin, Ireland; 2012. p. 1–6.

[5] Barrie, JV, Conway, KW. Seabed characterization for the development of marine renewable energy on the Pacific margin of Canada. Continental Shelf Res 2013;83(15):45–52.

[6] Cuellar P, Mira P, Pastor M, Fernandez Merodo JA, Baessler M, Ruecker W. A numerical model for the transient analysis of offshore foundations under cyclic loading. Computers and Geotechnics 2014;59:75–86.

[7] Stickle MM, De La Fuente P, Oteo C, Pastor M, Dutto P. A modelling framework for marine structure foundations with example application to vertical breakwater seaward tilt mechanism under breaking wave loads. Ocean Eng 2013;74:155–67.

[8] Seelig, WN. Direct embedment anchors. In: Thompson D, Beasley DJ, editors. SP-2209-OCN Handbook for Marine Geotechnical Engineering: Books Express Publishing; 2012, p. 6-1–6-42.

[9] Carnegie Wave Energy Limited. CETO technology. < http://carnegiewave.com/ceto-overview/>, 2015.

[10] Power-Technology.com. Pelamis, world's first commercial wave energy project, Agucadoura, Portugal. < http://www.power-technology.com/projects/pelamis/>, 2015.

[11] reNEWS Ltd. Swedes install wave power array. < http://renews.biz/72406/seabased-starts-swedish-wave-set/ >, 2015.

[12] Weller SD, Davies P, Vickers AW, Johanning L. Synthetic rope responses in the context of load history: operational performance. Ocean Eng 2014;83:111–24.

[13] Bahaj AS, Myers LE. Shaping array design of marine current energy converters through scaled experimental analysis. Energy 2013;59:83–94.

[14] Neill SP, Jordan JR, Couch SJ. Impact of tidal energy converter (TEC) arrays on the dynamics of headland sand banks. Renew Energy 2012;37:387–97.

[15] Damgaard M, Zania V, Andersen LV, Ibsen LB. Effects of soil-structure interaction on real time dynamic response of offshore wind turbines on monopiles. Eng Structures 2014;75:388–401.

[16] Low Carbon Innovation Coordination Group. Technology innovation needs assessment (TINA) marine energy summary report. http://www.lowcarboninnovation.co.uk/document.php?o=7>, 2012.

[17] Meggitt DJ, Jackson E, Machin J, Taylor R. Marine micropile anchor systems for marine renewable energy applications. In: Proceedings of the OCEANS Conference. San Diego, CA; 2013. p. 1–7.

[18] Det Norske Veritas. Environmental conditions and environmental loads. Recommended Practive DNV-RP-C205; 2010, pp. 124.

[19] Det Norske Vertia. Design of offshore steel structures, general (LRFD method). Offshore Standard DNV-OS-C101; 2011, pp. 73.

[20] Faltinsen OM. Sea loads on ships and offshore structures. Cambridge, UK: Cambridge University Press; 1998.

[21] Roald L, Chokani N, Jonkman J, Roberston A.The effect of second-order hydrodynamics on floating offshore wind turbines. Energy Procedia 2013;35:253–64.

[22] Johanning L, Smith GH, Wolfram, J. Measurements of static and dynamic mooring line damping and their importance for floating WEC devices. Ocean Eng 2007;34:1918–34.

[23] Chakrabarti S. Ocean environment. In: Chakrabarit SK, editor. Handbook of offshore engineering, Oxford, UK: Elsevier Ltd; 2005, p. 79–131.

[24] Wilkinson, L, Doherty, K, Henry, A, Whittaker, T, Day, S. Wave Loads on the Foundation of a Bottom-Hinged Modular Flap Structure. Proceedings of the International Conference on Offshore Renewable Energy, Glasgow, Scotland; 2014.

[25] Stansby PK, Devaney LC, Stallard, TJ. Breaking wave loads on monopiles for offshore wind turbines and estimation of extreme overturning moment, IET Renew Power Generation 2013;7:514–20.

[26] Petersen, TU. Scour around Offshore Wind Turbine Foundations. PhD Thesis, Technical University of Denmark; 2014.

[27] Arany, L, Bhattacharya, S, Macdonald, J, Hogan, SJ. Simplified critical mudline bending moment spectra of offshore wind turbine support structures. Wind Energy 2014;**18**(12):2171–2197.

[28] Gueydon S, Weller S. Study of a floating foundation for wind turbines. Journal of Offshore Mechanics and Arctic Eng-Transactions of the ASME 2013:135.

[29] EquiMar. Equitable testing and evaluation of marine energy extraction devices in terms of performance, cost and environmental impact. Edinburgh, UK: University of Edinbrugh; 2012.

[30] Det Norske Veritas. Position mooring. Offshore Standard DNV-OS-E301; 2013, pp. 101.

[31] Bureau Veritas. Current and tidal turbines. Guidance Note NI 603 DT R01 E; 2015.

[32] Det Norske Veritas. Design of offshore wind turbine structures. Offshore Standard DNV-OS-J101; 2014, pp. 238.

[33] Westphalen J, Greaves DM, Raby A, Hu ZZ, Causon DM, Mingham CG, Omidvar P, Stansby PK, Rogers BD. Investigation of wave-structure interaction using state of the art CFD techniques. Open Journal of Fluid Dynamics 2014;4:18–43.

[34] De Backer B, Vantorre M, Frigaard P, Beels C, De Rouck J. Bottom slamming on heaving point absorber wave energy devices. Journal of Marine Science and Technology 2010;15:119–130.

[35] Bahaj AS, Molland AG, Chaplin R, Batten WMJ. Power and thrust measurements of marine current turbines under various hydrodynamic flow conditions in a cavitation tunnel and a towing tank. Renew Energy 2007;32:407–26.

[36] Afgan, I, McNaughton J, Rolfo S, Apsley DD, Stallard T, Stansby, P. Turbulent flow and loading on a tidal stream turbine by LES and RANS. International Journal of Heat and Fluid Flow 2013;43:96–108.

[37] Weller, SD, Stallard, TJ, Stansby, PK. Experimental measurements of irregular wave interaction factors in closely spaced arrays. IET Renew Power Generation 2010;4:628–37.

[38] Stratigaki, V, Troch, P, Stallard, T, Forehand, D, Kofoed, JP, Folley, M, Benoit, M, Babarit, A, Kirkegaard, J. Wave basin experiments with large wave energy converter arrays to study interactions between the converters and effects on other users in the sea and the coastal area. Energies 2014;7:701–34.

[39] Babarit, A. On the park effect in arrays of oscillating wave energy converters. Renew Energy 2013;58:68–78.

[40] Vicente, PC, Falcaoa, AFDO, Gato, LMC, Justino, PAP. Dynamics of arrays of floating point-absorber wave energy converters with inter-body and bottom slack-mooring connections. Appl Ocean Res 2009;31:267–81.

[41] Gao, Z, Moan, T. Mooring system analysis of multiple wave energy converters in a farm configuration. In: Proceedings of the 8th European Wave and Tidal Energy Conference. Uppsala, Sweden; 2009.

[42] Vaitkunaite, E, Ibsen, LB, Nielsen, BN, Molina, SD. Comparison of foundation systems for wave energy converters Wavestar. In: Proceedings of the 10th European Wave and Tidal Energy Conference. Aalborg, Denmark; 2013.

[43] Johanning, L, Thies, PR, Parish, D. Smith, GH. Offshore reliability apporach for floating renewable energy devices. Proceedings of the International conference on Offshore Mechanics and Arctic Engineering. Rotterdam, The Netherlands; 2011.

[44] Gordelier, T, Parish, D, Johanning, L. A novel mooring tether for highly dynamic offshore applications; mitigating peak and fatigue loads via selectable axial stiffness. In: Proceedings of the International Conference on Offshore Renewable Energy. Glasgow, UK; 2014.

[45] Rodríguez, A, Weller, SD, Canedo, J, Rodríguez, R, González de Lena V, Thies PR, Parish D, Johanning L, Leao A. Performance comparison of marine renewable energy converter mooring lines subjected to real sea and accelerated loads. In: Proceedings of the 11th European Wave and Tidal Energy Conference. Nantes, France; 2015.

[46] Harnois, V, Thies, PR, Johanning, L. On Peak Mooring Loads and the Influence of Environmental Conditions for Marine Energy Converters. Journal of Marine Science and Engineering 2016;4(2):29.

[47] Smith, HCM, Ashton, IGC, Van-Nieuwkoop, J, Parish, D, Johanning, L. Wave resource assessment for the Falmouth Bay marine energy test site (FaBTest). Proceedings of the 4th International Conference on Ocean Energy, Dublin, Ireland; 2012.

[48] Sjolte, J, Tjensvoll G, Molinas M. Power collection from wave energy farms. Appl Sciences 2013;3:420–36.

[49] S.D. Weller, P. Davies, A.W. Vickers, L. Johanning, Synthetic rope responses in the context of load history: the influence of aging, Ocean Eng 96 (2014) 192-204.

[50] Brodtkorb, PA, Johannesson, P, Lindgren, G, Rychlik, I, Ryden, J, Sjo, E. WAFO—A Matlab toolbox for analysis of random waves and loads. In: Chung JS, Olagnon M, Kim CH, editors. Proceedings of the 10th International Offshore and Polar Engineering Conference. Seattle, USA; 2000. p. 343–350.

[51] Thompson, D, Beasley, DJ. SP-2209-OCN Handbook for Marine Geotechnical Engineering. Books Express Publishing; 2012.

[52] James, NP, Dalrymple, RW. Facies model 4. St. John's, Newfoundland and Labrador, Canada: Geological Association of Canada, 2010. pp. 586.

[53] OzCoasts Australia. Evolution of Australian estuaries and coastal waterways. < http://www.ozcoasts.gov.au/conceptual_mods/geomorphic/evolution.jsp>, 2013.

[54] Heath, J, Jensen, R, Arguello Jr J, Roberts, J, Bull, D, Weller, S, Hardwick, J, Johanning, L. Deliverable 4.2: Specific requirements for MRE foundation analysis. Optimal Design Tools for Ocean Energy Arrays (DTOcean) project report, < http://www.dtocean.eu/Deliverables-Documentation/Deliverables/Deliverable-4.2 >,2014. pp. 43.

[55] Kelkar, M, Perez, G, Anil, C. Applied geostatistics for reservoir characterization. Society of Petroleum Engineers 2002. pp. 264.

[56] Goff, JA, Kraft, BJ, Mayer, LA, Schock, SG, Sommerfield, CK, Olson, HC, Gulick, SPS, Nordfjord, S. Seabed characterization on the New Jersey middle and outer shelf: correlatability and spatial variability of seafloor sediment properties. Marine Geology 2004;209:147–72.

[57] Chen, L, Lam, WH. Methods for predicting seabed scour around marine current turbine. Renew Sustain Energy Rev 2014;29:683–92.

[58] Stallard, T, Feng, T, Stansby, PK. Experimental study of the mean wake of a tidal stream rotor in a shallow turbulent flow. Journal of Fluids and Structures 2015;34:235–46.

[59] Gerolymos, N, Gazetas, G. Constitutive model for 1-D cyclic soil behaviour applied to seismic analysis of layered deposits. Soils Found 2005;45:147–59.

[60] Oka, F, Kodaka, T, Kim, YS. A cyclic viscoelastic-viscoplastic constitutive model for clay and liquefaction analysis of multi-layered ground. International Journal of Numerical Analytical Methods in Geomechanics 2004;28:131–79.

[61] Zienkiewicz, OC, Chang, CT. Bettess, P. Drained, undrained, consolidating and dynamic behavior assumptions in soils. Geotechnique 1980;30:385–95.

[62] Cuellar, P, Baessler, M, Rucker, W. Relevant factors for the liquefaction susceptibility of cyclically loaded offshore monopiles in sand. In: Poromechanics V. Proceedings of the Fifth Biot Conference on Poromechanics. Vienna, Austria; 2013. p. 1336–45.

[63] Abelev, A, Simeonov, J, Valent, P. Numerical investigation of dynamic free-fall penetrometers in soft cohesive marine sediments using a finite element approach. In: Proceedings of the OCEANS Conference.Biloxi, MS; 2009.p. 1–8.

[64] Hu, C, Liu, H. Implicit and explicit integration schemes in the anisotropic bounding surface plasticity model for cyclic behaviours of saturated clay. Computers and Geotechnics 2014;55:27–41.

[65] Hu, C, Liu, HX, Huang, W. Anisotropic bounding-surface plasticity model for the cyclic shakedown and degradation of saturated clay. Computers and Geotechnics 2012;44:34–47.

[66] Katti, DR, Desai, CS. Modeling and testing of cohesive soil using disturbed-state concept. Journal of Eng Mechanics 1995;121:648–58.

[67] Lu, Q, Randolph, MF, Hu, Y, Bugarski, IC. A numerical study of cone penetration in clay. Geotechnique 2004;54:257–67.

[68] Walker, J, Yu, HS. Adaptive finite element analysis of cone penetration in clay. Acta Geotechnica 2006;1:43–57.

[69] Wang, JH, Li, C, Moran, K. Cyclic undrained behavior of soft clays and cyclic bearing capacity of a single bucket foundation. In: Proceedings of the 15th International Society Offshore and Polar Engineering. Seoul, Korea; 2005. p. 392–99.

[70] Wu K, Ma M, Chen R. Numerical analysis of cyclic bearing capacity of suction bucket foundation based on elasto-plastic FEM. Electronic Journal of Geotechnical Engineering 2010;15B:1–13.

[71] Tekeste MZ, Raper RL, Tollner EW, Way TR. Finite element analysis of cone penetration in soil for prediction of hardpan location. Trans of the ASABE 2007;50:23–31.

Figures

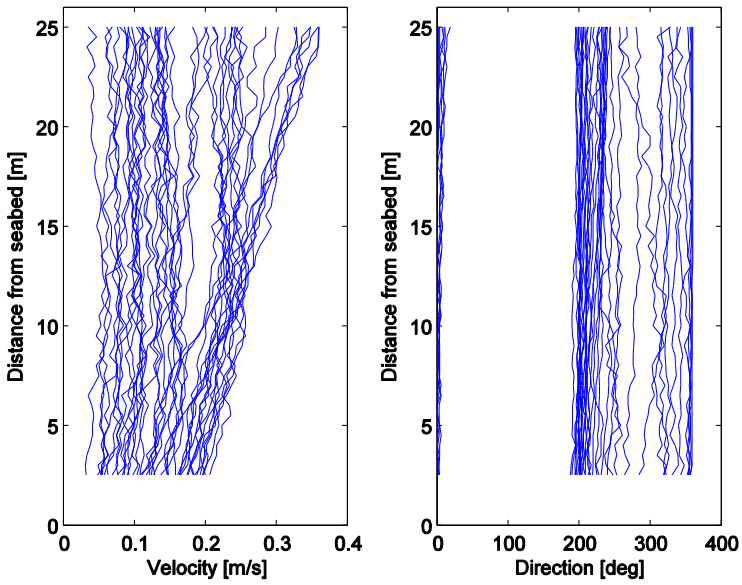

Fig. 1. Acoustic doppler current profiler (ADCP) measurements recorded during one tidal cycle (21/12/2010) at the South West Mooring Test Facility (SWMTF) test site. The results shown are based on averaging data at 17 minute intervals.

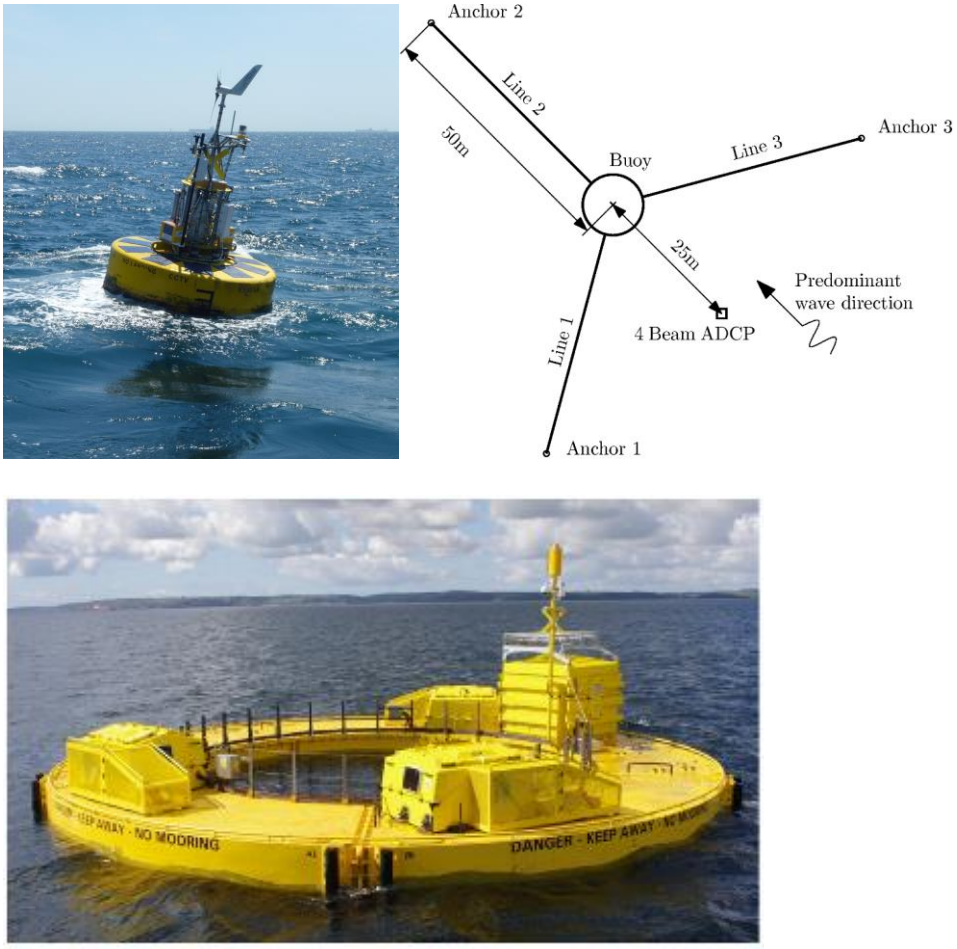

Fig. 2. Field examples of systems to test loads related to MRE devices. (a) South West Mooring Test Facility (SWMTF), (b) SWMTF mooring configuration [12], and (c) Fred Olsen BOLT Lifesaver device.

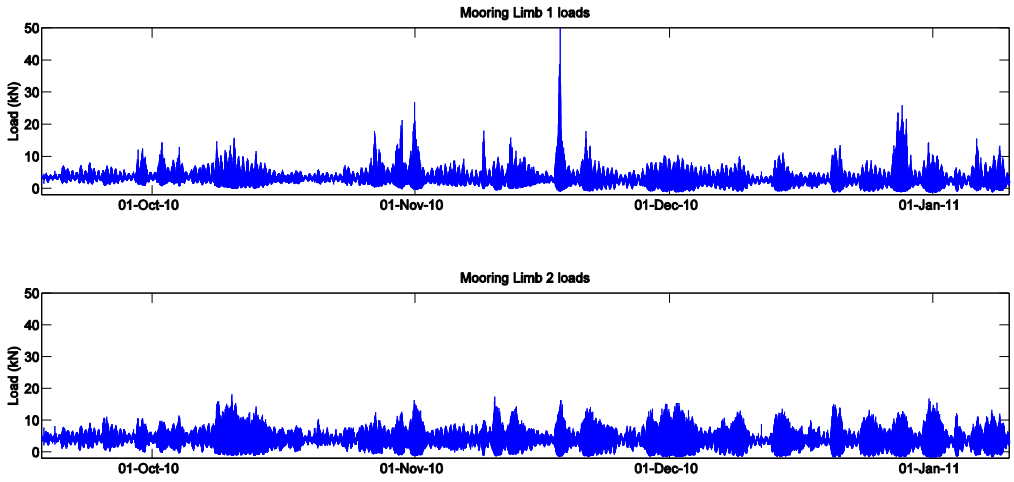

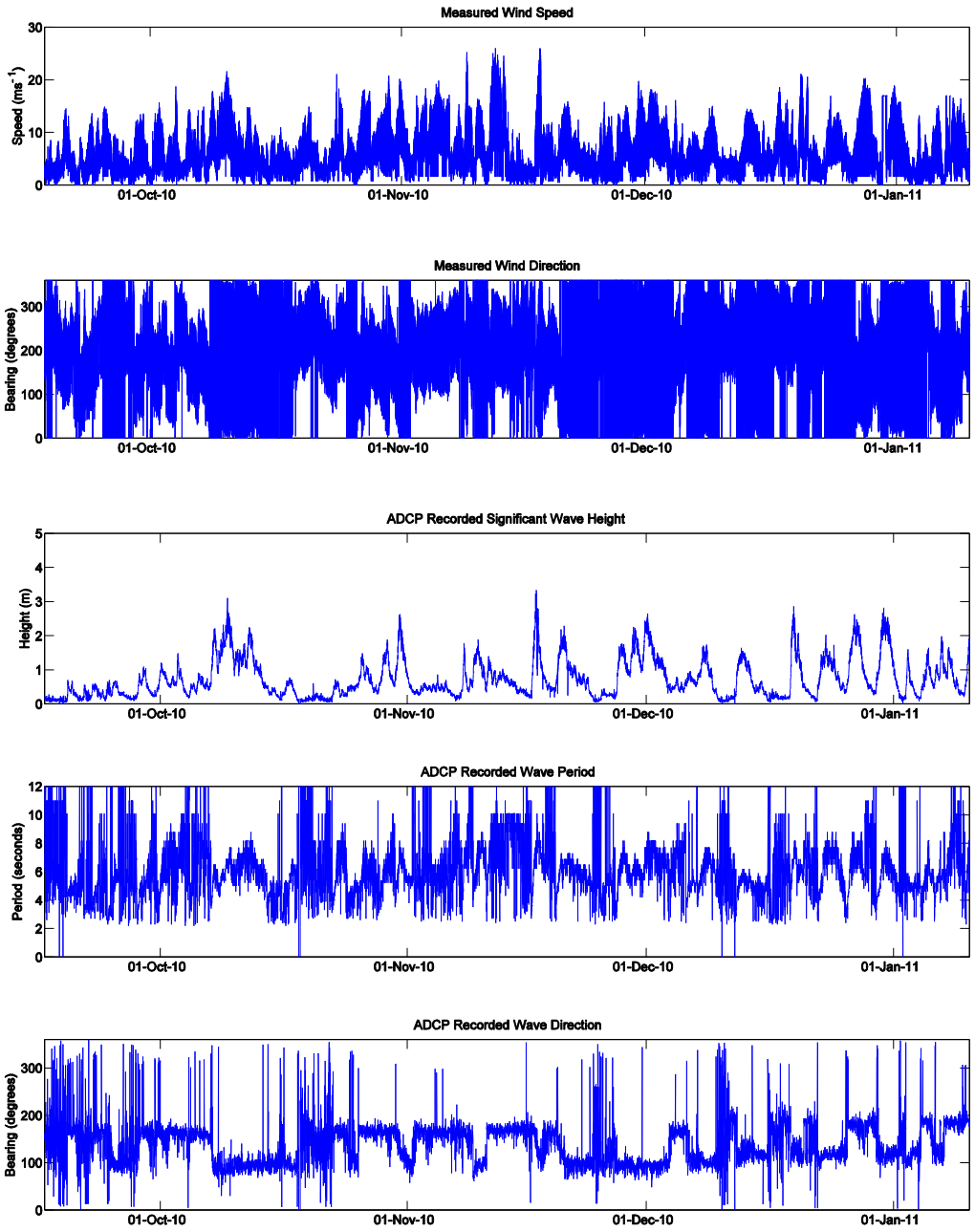

Fig. 3. Time series showing loads measured by the SWMTF on mooring limb 1 (a) and 2 (b), the wind speed (c) and wind direction (d) measured from the SWMTF buoy, Hs (e), Tp (f) and wave direction (g) measured from the ADCP located 25 m from the buoy.

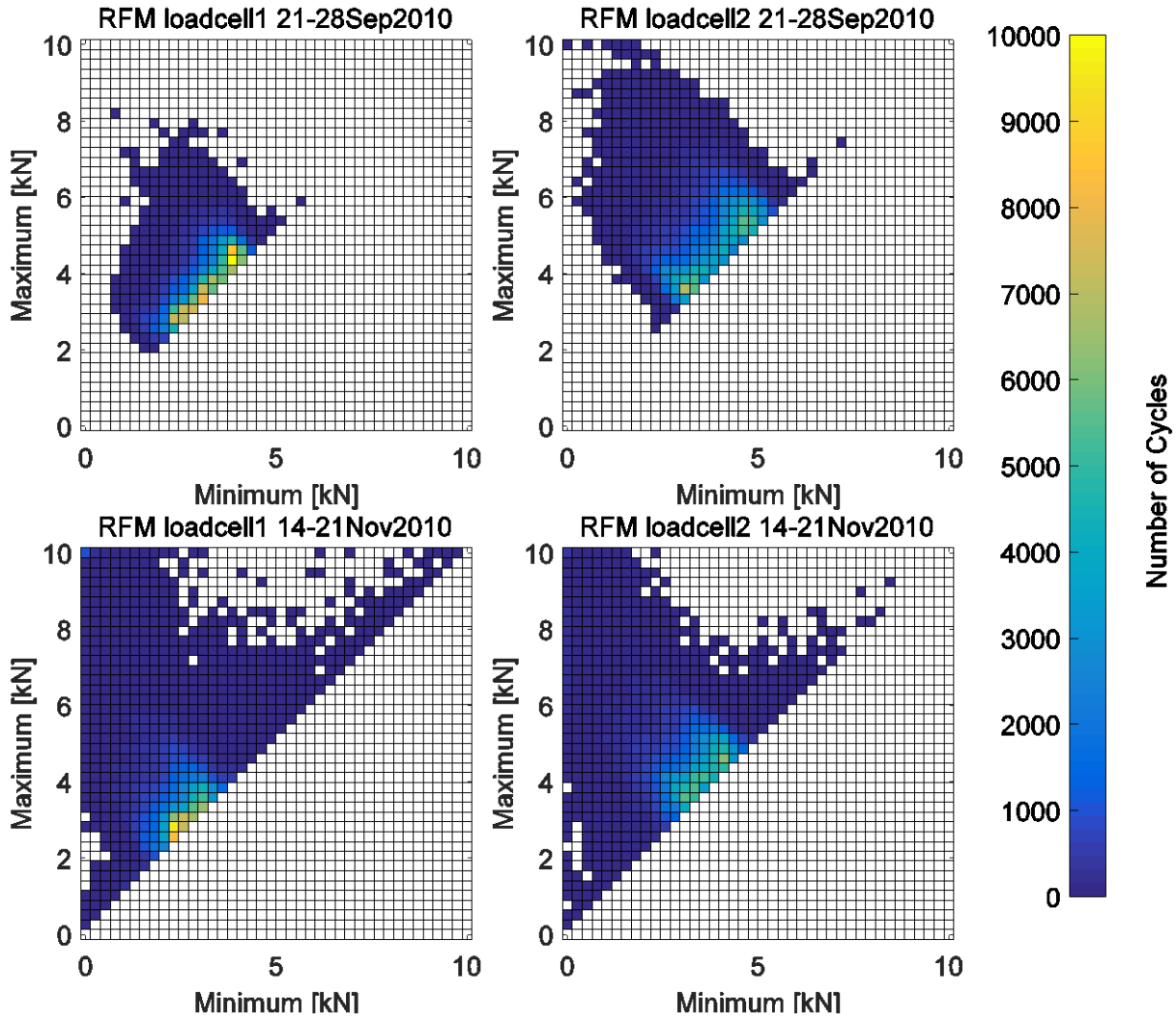

Fig. 4. Rainflow diagrams of mooring tensions measured by lines 1 and 2 of the SWMTF.

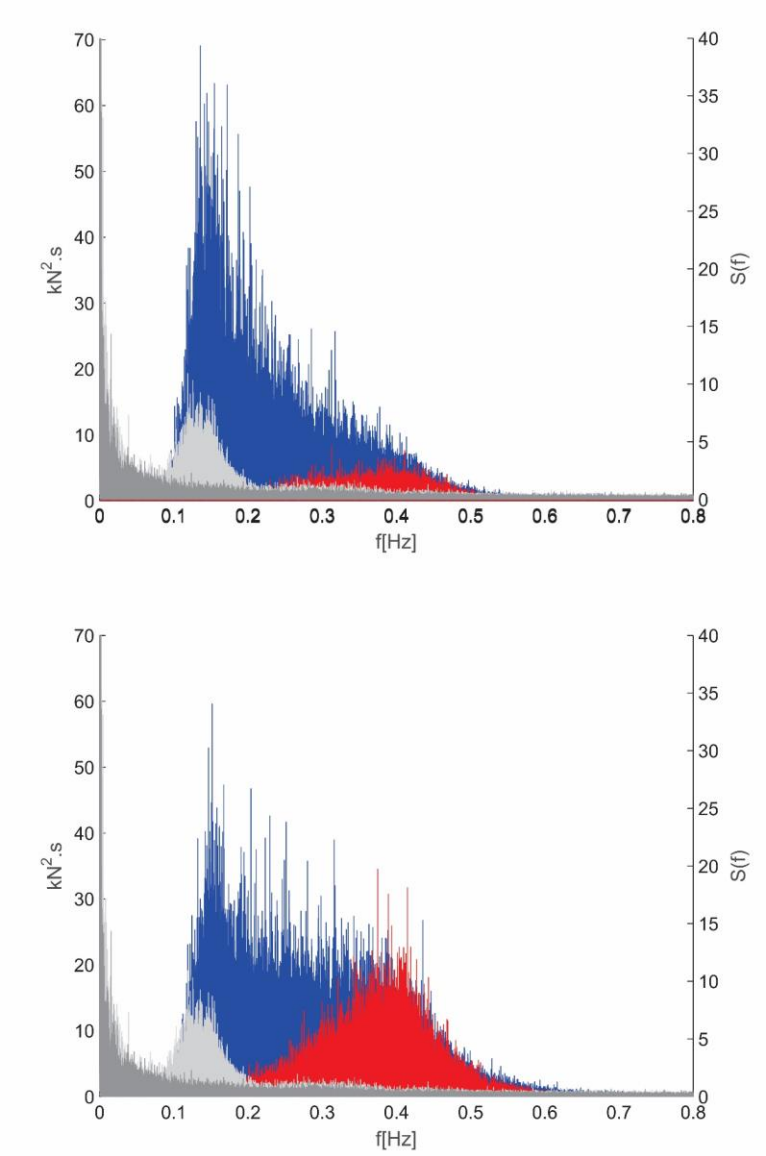

Fig. 5. Spectral distribution of mooring line tensions for (a) line 1 and (b) line 2 measured between 21–26 September 2010 and 14–21 November 2010 (red and blue lines respectively). Spectra calculated from the surface elevation time-series are shown for the intervals 21–26 September 2010 (dark grey) and 14–21 November 2010 (light grey).

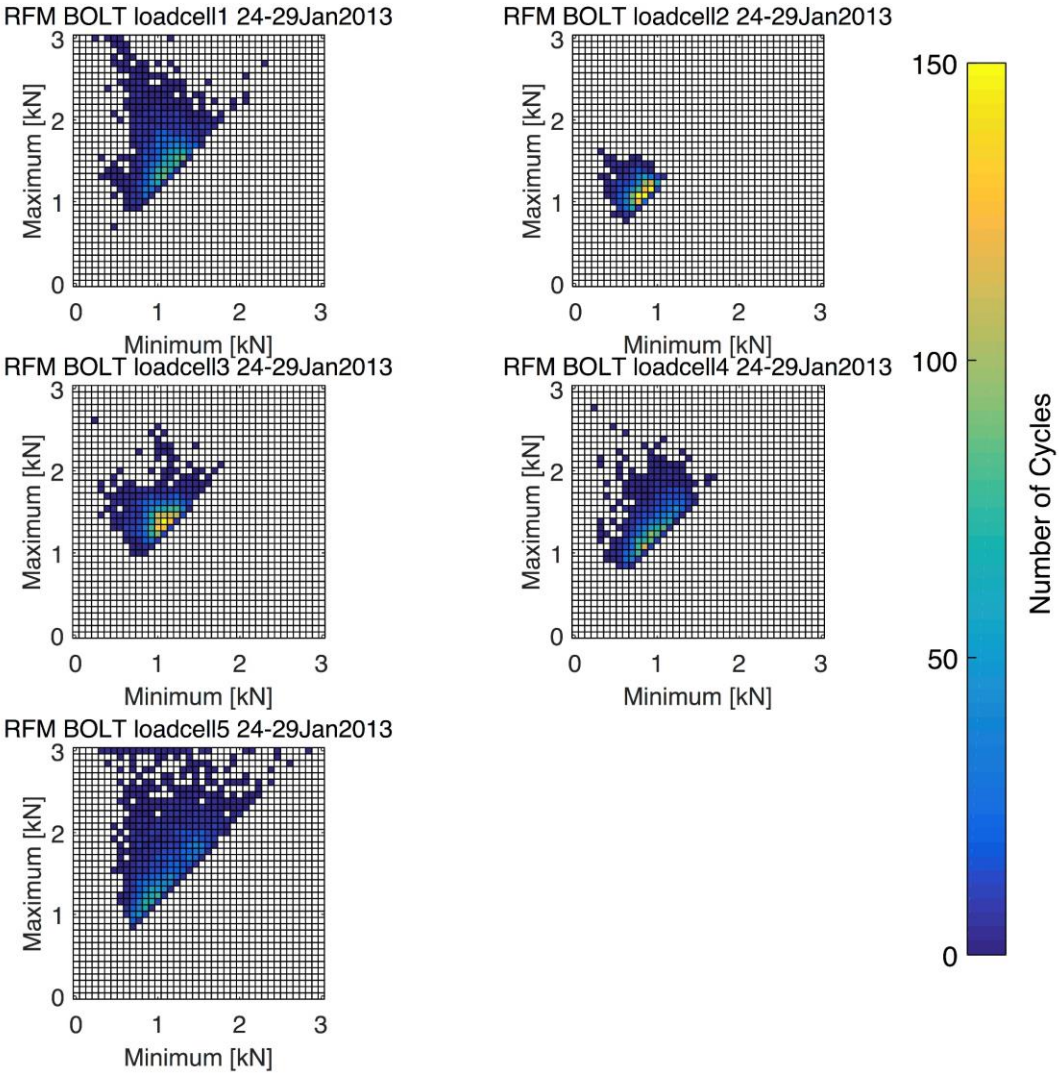

Fig. 6. Rainflow matrix diagrams of the mooring tensions on each of the five mooring lines on the Fred Olsen BOLT device.

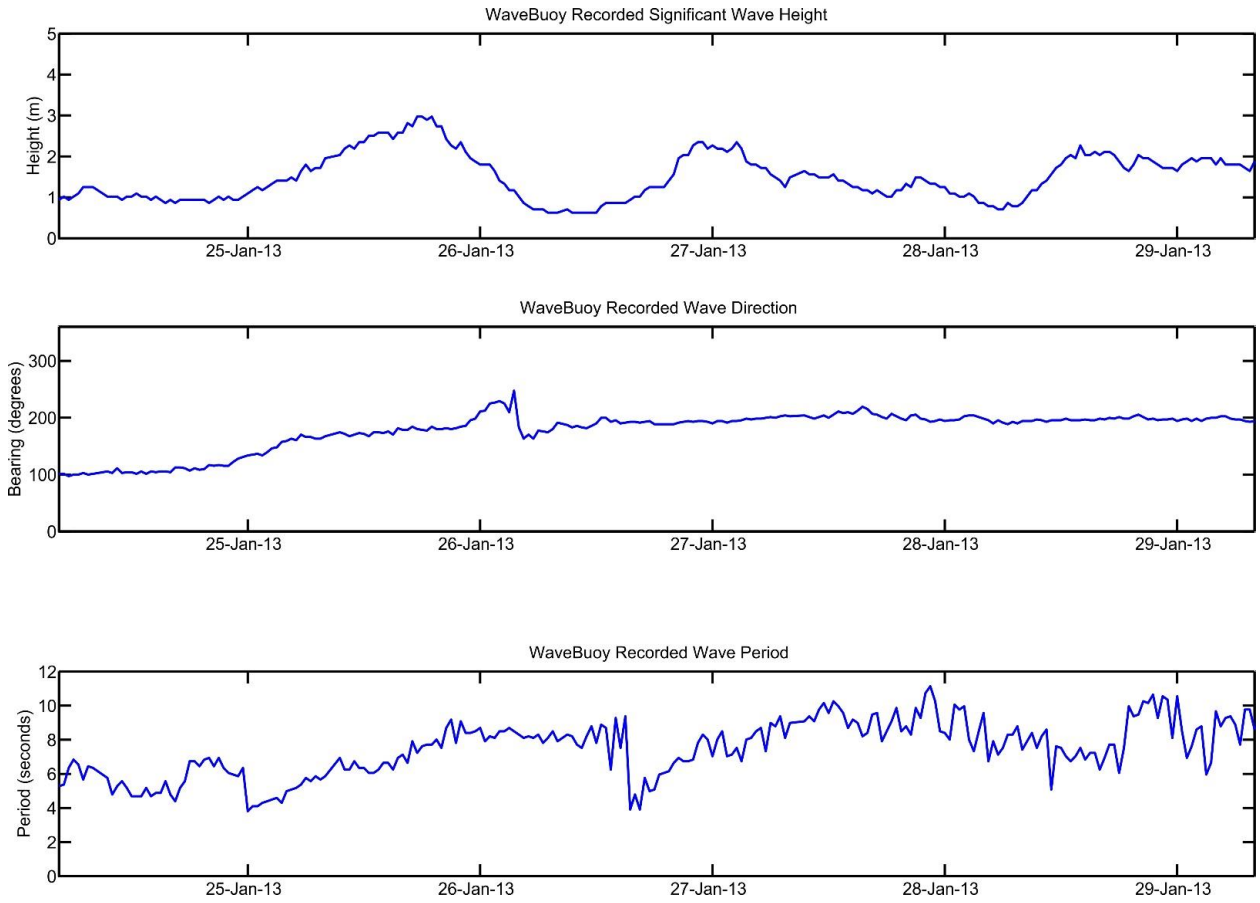

Fig. 7. Hs (a), Tp (b) and direction (c) recorded from the University of Exeter wave buoy located at the FabTest site close to the BOLT device.

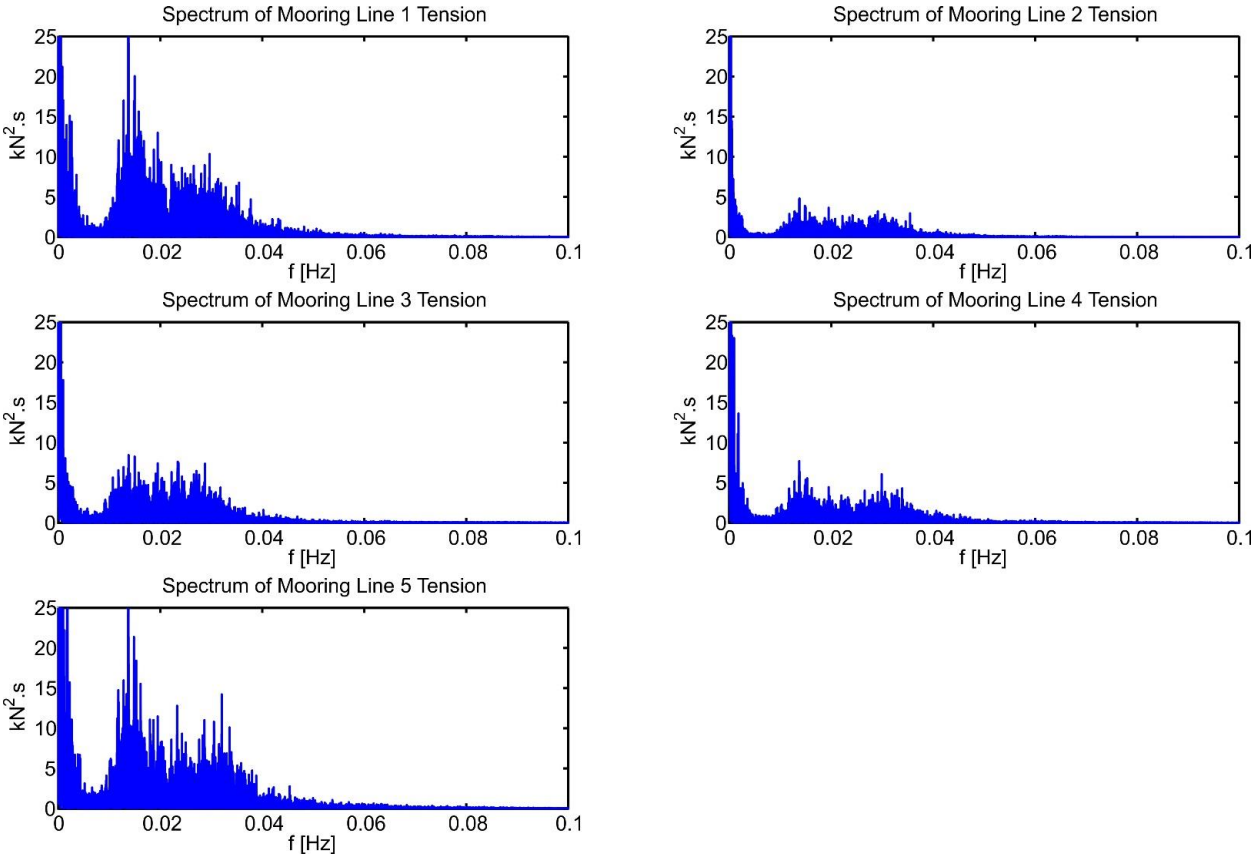

Fig. 8. Spectral distribution of the mooring line tensions from the Fred Olsen BOLT Lifesaver device for the interval 24–29 January 2013.

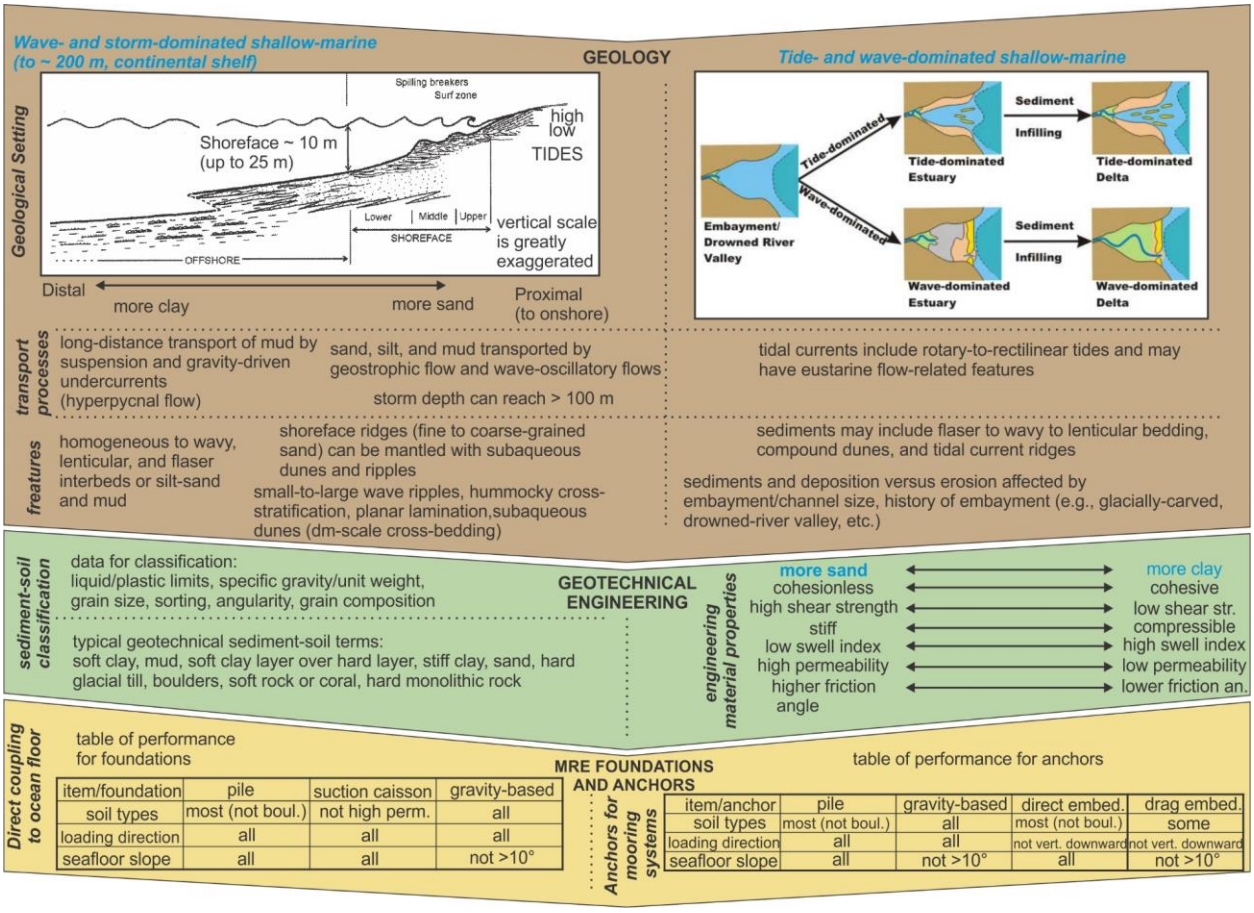

Fig. 9. Schematic of the influence of geological and geotechnical properties of seafloor materials and performance of MRE foundations and anchors. Upper left image is adapted from [52]. Upper right image is from [53]. Figure is from [54].

Tables

Table 1
Categorized loading sources that may be experienced by MRE device mooring and foundation systems

Loading type	Example load sources	
Static	• Mooring line pretension • Steady wind	• Steady current • Mean wave drift
Cyclic	• Wave loading (first-, second- and higher-order) • Tidal cycles	• Tidal turbulence • Power take-off harmonics
Impulse	• Wave slamming or breaking • Wind gusts • Seismic disturbances	• Ice flows • Marine life • Snatch loading

Table 2
Number of significant load cycles and peak loads measured by mooring lines 1 and 2 during the two intervals of interest

Line	Date range	Hs (m)	Tp (s)	Peak load (kN)	Number of cycles > 0.2kN
1	21-26/09/2010	0.06-0.7	2.2-16.8	8.11	210996
	14-21/11/2010	0.15-3.34	2.5-16.8	52.48	182891
2	21-26/09/2010	0.06-0.7	2.2-16.8	11.06	242365
	14-21/11/2010	0.15-3.34	2.5-16.8	16.35	214163

Table 3
Typical loading regimes experienced by fixed and floating MRE devices (from [54])

		Wave Energy Arrays		Tidal Stream Arrays	
		Fixed	**Floating**	**Fixed**	**Floating**
Frequent	Turbine rotation and blade passing frequencies			✓	✓
	Power Take-off and gearbox harmonics	✓	✓	✓	✓
	Wave / Tidal loading	✓	✓	✓	✓
	Wind loading	✓	✓	✓*	✓*
	Ice loading (location dependent)	✓	✓	✓	✓
	Anchor line pick-up and drop		✓		✓
	Irregular loading at shared connection points / foundations / anchors	✓	✓	✓	✓
Infrequent	Turbulence (eddies and surges)	✓	✓	✓	✓
	Steep waves / storms	✓	✓	✓*	✓*
	Tidal velocity extremes	✓	✓	✓	✓
	Wave slamming	✓	✓	✓*	✓*

Seismic activity	✓		✓	
Wind gusts	✓	✓	✓*	✓*
Impact from vessels / marine life / ice flows	✓	✓	✓	✓
Effect of anchor displacement and re-embedment (drag anchors only)		✓		✓
Snatch loading at shared connection points		✓		✓
Load and device response amplification due to hydrodynamic interactions between devices	✓	✓	✓	✓

*Loads relevant for surface piercing structures or devices are indicated with an asterisk.

Table 4
Constitutive relations applicable to marine sediments (from [54])

Constitutive Models	Material	Features	Comments on Cyclic Loading	Ref.
Bounding surface plasticity model	marine clay, over to underconsolidated	bounding surface models (isotropic and kinematic hardening rules; applied in ABAQUS (see [65])	captures cyclic behaviors: cyclic shakedown and strength degradation; initial anisotropy; 8 material property parameters, obtainable from lab tests	[64, 65]
BWGG	cohesive soil	1D, static/dynamic response; reproduces complex non-linear behaviors: cyclic mobility; liquefaction; stress-strain loops; pore-water pressure buildup; example not found for modern MRE systems	reproduces stiffness and strength degrading behavior due to cyclic loading; may require in situ or lab cyclic triaxial and cyclic simple shear tests for parameterization; 3 parameters to capture experimental modulus decline and damping growth versus shear strain curve	[59]
Disturbed-state concept (DSC)	saturated cohesive (clay-bearing) soils	inelastic response during loading (virgin) and unloading-reloading (non-virgin) behavior; drained and undrained behavior and pore water pressure	accommodates cyclic loading; 15 parameters, (intact state, critical state, disturbance parameters, nonvirgin parameters); parameterization may include cyclic cylindrical triaxial and truly triaxial devices	[66]
Drucker-Prager	sand, clay	plastic deformation; cone penetration examples include von Mises yield crierion with assoicated flow rule; implemented in ABAQUS; large displacement	our literature search not yet found on direct examples for cyclic loading; cone penetration examples are relevant	[68, 71]
Elastoplastic	soft cohesive marine soils	literature includes von Mises plastic or Tresca yield criterion for marine applications; can incorporate depth dependent shear strength; solved with ABAQUS and Arbitrary Lagrangian-Eulerian	can be applied to cyclic loading (see Wu et al., 2004); number of cycles very important on ultimate bearing capacity; some applications, e.g., cone penetration test, not applicable to cyclic loading and more for large-strain problems	[63, 67, 69, 70]
Elasto-viscoplastic based on Cam-Clay model	clay/sand, layered material	elasto-viscoplastic for normally consolidated clay, based on Cam-Clay model and the extension of an overstress-type viscoplasticity; previously used for earthquake applications; low to high level strain; IQCA-2D, effective stress-based liquefaction code	obtains cyclic loading and possible liquefaction for sand/clay layering	[60]
Generalized plasticity framework	sand ([7])	isotropic material response for granular soil behavior under monotonic and cyclic loading, non-linear elastic soil response; captures critical state condition, dilative response after peak, liquefaction in loose sands, memory of previous stress path, plastic modulus	handles cyclic loadings and complex foundation-structure interaction; SandPZ suited for water-soil and water-structure and structure-soil interfaces; 13 material parameters requiring definition; need monotonic and cyclic triaxial tests in general	[7]

Table 5
Constitutive models with information on parameters and in situ or laboratory testing (from [54])

Constitutive model	Constitutive model parameters[1]	Obtaining parameters	Ref.
Bounding surface plasticity	8 parameters critical state soil mechanics (λ, κ, M, G, or ν)1 hardening modulus (γ, ζr, η, β)	critical state parameters from in situ or lab tests; tests may include isotropic consolidation including critical state lines in extension and compression; monotonic element tests hardening from trial and error modeling of lab results of undrained monotonic shearing and undrained cyclic triaxial tests; reloading and unloading cycles needed for ζr and η	[65]
BWGG	parameters for shear modulus and damping curves shear modulus, undrained shear strength, parameters for hysteretic nonlinear response of sediment, and others (see reference as the parameters are not presented in the reference for ready enumeration here)[2]	lab tests including cyclic triaxial and cyclic simple shear; reloading and unloading curves needed in situ tests including standard penetration (SPT) and the crosshole centrifuge or shaking table sediment response	[59]
Disturbed-state concept	15 parameters two for elasticity (E, ν) five for $\delta 0$ model (γ, β, n, h1, h2) two for critical state (m', λ), two for disturbance function (A, Z) four for non-virgin loading (K_1,K_2,β^{UL},β^{RL})	lab testing includes loading-unloading-reloading stress paths include conventional triaxial compression, reduced triaxial compression, and cyclic; shear tests include consolidated undrained with pore-water-pressure measurements; reference discusses cylindrical and cubical samples (for truly triaxial testing)	[66]
General Plasticity	13 parameters dimensionless parameters involving initial bulk modulus, initial mean effective stress, initial shear modulus, the exponent for non-linear elastic stiffness, fitting shape of stress path in undrained triaxial test, fitting for number of cycles in a series of loading-reloading, and others (see reference for full details)	generally obtained from lab tests, including monotonic and cyclic triaxial tests	[7]

[1]See reference for definition of parameters, especially for those given here with symbols

[2]Note that full methodology for parameter identification is not included in the reference for this constitutive model